

Cite this: *J. Mater. Chem. A*, 2024, 12, 13682Received 11th March 2024  
Accepted 15th May 2024

DOI: 10.1039/d4ta01653j

rsc.li/materials-a

# A green oxidizer based on 1,2,3-triazole with a high oxygen balance of +23.3%: a promising replacement of ammonium perchlorate in solid propellants†

Pinxu Zhao,<sup>ab</sup> Long Chen,<sup>b</sup> Qingzhong Zhang,<sup>b</sup> Yifei Ling,<sup>b</sup> Qiuhan Lin,<sup>ID</sup>\*<sup>a</sup>  
Haifeng Huang<sup>ID</sup>\*<sup>b</sup> and Jun Yang<sup>ID</sup>\*<sup>b</sup>

A novel 1,2,3-triazole-based green oxidizer 4-nitro-2,5-bis(trinitromethyl)-1,2,3-triazole (**JY-23**) with high oxygen balance (OB<sub>CO<sub>2</sub></sub> = +23.3%) was synthesized in 5 steps from 4-cyano-5-nitro-1*H*-1,2,3-triazole. Its structure was confirmed by NMR, IR, elemental analysis and single crystal X-ray diffraction. It exhibits a high density (1.931 g cm<sup>-3</sup>), a high positive enthalpy of formation ( $\Delta_f H = +294.81$  kJ mol<sup>-1</sup>), and acceptable mechanical sensitivities (IS = 11 J and FS = 42 N), and, importantly, it is non-hygroscopic. The contribution of **JY-23** to the specific impulse of solid propellants as a replacement for ammonium perchlorate (AP) in typical HTPB (hydroxyl terminated polybutadiene) and GAP (glycidyl azide polymer) solid propellants was calculated using NASA-CEA software. The results show that the replacement of AP with **JY-23** results in a much higher specific impulse compared to some previously reported oxidizers, suggesting its potential application as a green oxidizer to replace AP in solid propellants.

Polynitro compounds based on nitrogen-rich heterocyclic rings are of great significance in the development of high energy density oxidizers (HEDOs) due to their chlorine-free properties, high density and positive oxygen balance.<sup>1,2</sup> The main strategy for designing an oxidizer with good performances is to combine the skeleton with oxygen-rich groups.<sup>3</sup> Triazole rings including 1,2,3-triazole and 1,2,4-triazole are second only to tetrazole in nitrogen content and enthalpy of formation, but they have more reaction sites, stronger modifiers and better stability, making them ideal skeletons for development of HEDOs.<sup>4</sup> Among them, 1,2,3-triazole ( $\Delta_f H = 262.8$  kJ mol<sup>-1</sup>) has higher enthalpy of

formation than 1,2,4-triazole ( $\Delta_f H = 192.7$  kJ mol<sup>-1</sup>). Additionally, the oxygen balance is an important criterion for determining oxygen excess or deficiency in energetic compounds. A qualified oxidizer for propellants, whose primary function is to provide sufficient oxygen to meet the oxygen demand for the combustion of the propellant, should have a high oxygen balance.<sup>5,6</sup> The introduction of oxygen-rich groups including nitro, nitramine, dinitromethyl and trinitromethyl groups is the key approach to improve oxygen balance. The introduction of more nitro groups in energetic compounds can normally improve their oxygen balance and density; however, the introduction of too many nitro groups will possibly result in poor stability. Thus, developing new HEDOs with high oxygen balance and acceptable stabilities has long been a big challenge in the field of energetic materials.<sup>7-9</sup>

Over recent decades, many energetic compounds derived from 1,2,4-triazole and 1,2,3-triazole have been documented.<sup>10,11</sup> Compared with energetic compounds based on 1,2,3-triazole, more 1,2,4-triazole derived energetic compounds with positive oxygen balance have been reported, such as 5-(dinitromethyl)-3-(trinitromethyl)-1*H*-1,2,4-triazole (**II**),<sup>12</sup> 3-nitro-1-(trinitromethyl)-1*H*-1,2,4-triazole (**III**),<sup>13</sup> 1,3-bis(trinitromethyl)-1,2,4-triazole (**V**),<sup>14</sup> etc. Compound **VI** has a high balance of +20.8%, which is the highest among the 1,2,4-triazole derived energetic compounds (Fig. 1a). However, it exhibits poor chemical stability and decomposes at room temperature.<sup>15</sup> Although 1,2,3-triazole has higher energy and better symmetry than 1,2,4-triazole, the investigation of nitro-1,2,3-triazole energetic compounds with positive oxygen balance is restricted by the constrained synthesis of 1,2,3-triazole compounds.<sup>16,17</sup>

We are trying to introduce as many nitro groups as possible into the 1,2,3-triazole ring to achieve a higher oxygen balance. Drawing inspiration from previous work on nitro 1,2,4-triazole compounds, the combination of trinitromethyl groups with the triazole skeleton has resulted in a stable structure with high oxygen balance, excellent density and good stability (compound **V**). On this basis, by retaining trinitromethyl moieties and replacing 1,2,4-triazole with another nitro-triazole in the central

<sup>a</sup>School of Chemistry and Chemical Engineering, Nanjing University of Science and Technology, Xiaolingwei Road 200, Nanjing, 210094, P. R. China. E-mail: lingqh@njust.edu.cn

<sup>b</sup>Key Laboratory of Fluorine and Nitrogen Chemistry and Advanced Materials, Shanghai Institute of Organic Chemistry, Chinese Academy of Sciences, Lingling Road 345, Shanghai, 200032, P. R. China. E-mail: hfhuang@sioc.ac.cn; yangj@sioc.ac.cn

† Electronic supplementary information (ESI) available. CCDC 2256910. For ESI and crystallographic data in CIF or other electronic format see DOI: <https://doi.org/10.1039/d4ta01653j>



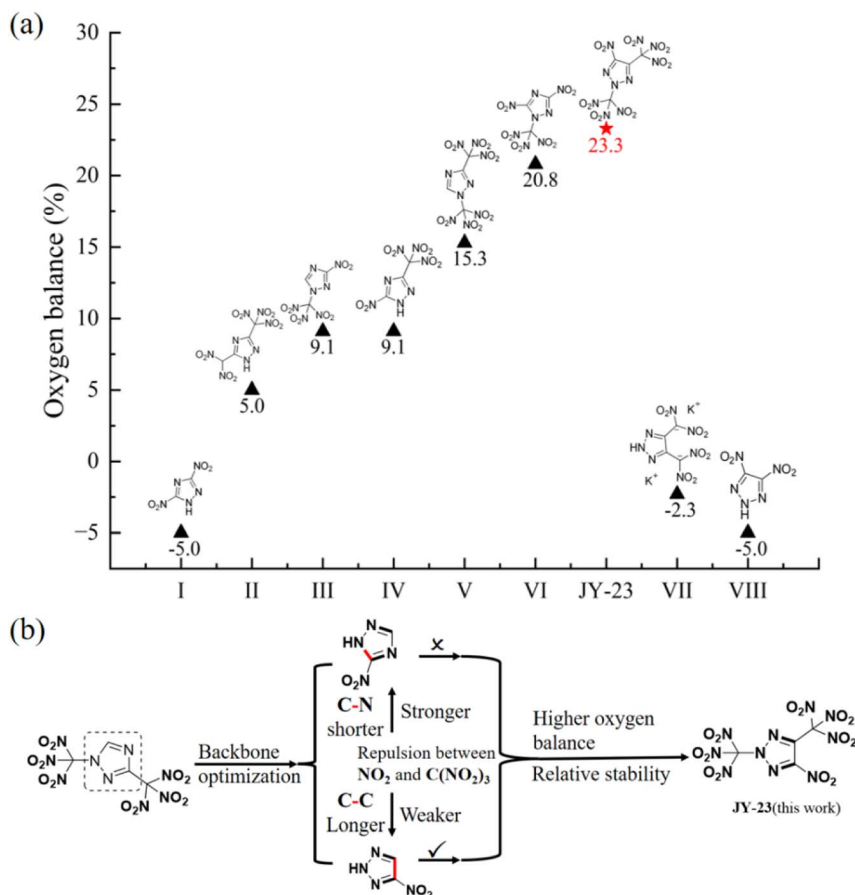


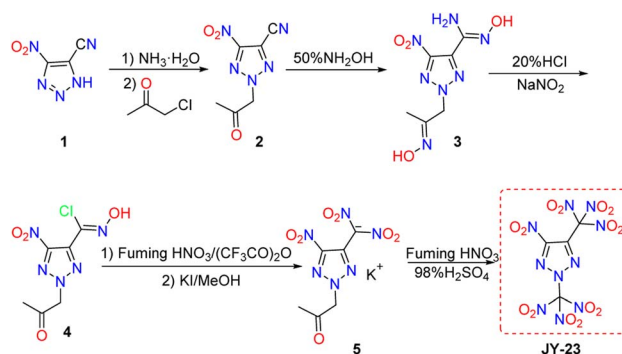
Fig. 1 (a) The oxygen balance comparison of JY-23 with other nitro-triazole compounds. (b) The design of molecular stability.

skeleton, a breakthrough in oxygen balance can be achieved. In order to avoid interference between molecular groups leading to poor stability, it is necessary to screen for an appropriate skeleton. Specifically, compound VI shows very poor chemical stability due to the strong repulsion between the nitro group and the *ortho*-trinitromethyl group. Hence, it may not be ideal to adjust the skeletal structure of compound V mentioned above to nitro-1,2,4-triazole.<sup>15</sup> As shown in Fig. 1b, the length of the C-C bond is comparatively longer than the length of the C-N bond; therefore on replacing the central skeleton with nitro-1,2,3-triazole, the repulsion between adjacent groups becomes weaker, and it is expected that a stable molecular structure will be obtained.

Based on the preceding discussion, the fully nitrated compounds of 1,2,3-triazole were achieved by merging the nitro-1,2,3-triazole skeleton with trinitromethyl groups. We have successfully synthesized 4-nitro-2,5-bis(trinitromethyl)-1,2,3-triazole (JY-23), which shows high oxygen balance, excellent density, and positive enthalpy of formation while maintaining good stability.

As shown in Scheme 1, the starting material 4-cyano-5-nitro-1H-1,2,3-triazole (**1**) can be easily synthesized according to the procedure specified in the literature.<sup>18,19</sup> Compound **1** was deprotonated with aqueous ammonia to produce the corresponding ammonium salt, which was then reacted directly with

chloroacetone in DMF to give the simple *N*-alkylation product **2**. The treatment of compound **2** with an aqueous hydroxylamine solution resulted in the oximation of the cyano group and the *N*-acetyl group to yield compound **3**. Subsequently, the Sandmeyer and deoximation reactions of compound **3** with hydrochloric acid (20% HCl) and NaNO<sub>2</sub> produced compound **4**. The nitration of compound **4** with fuming nitric acid and (CF<sub>3</sub>CO)<sub>2</sub>O followed by treatment with potassium iodide (KI) gave potassium salt **5**. Potassium salt **5** was nitrated using a mixture of fuming nitric acid and concentrated sulfuric acid to generate JY-



Scheme 1 Synthetic route of JY-23.



**23** as a non-hygroscopic white solid. The structure of **JY-23** was determined by standard analytical methods including single crystal X-ray diffraction.

The crystals suitable for single-crystal X-ray diffraction of **JY-23** were acquired through gradual evaporation of its methanol solution at room temperature. The structure is shown in Fig. 2. **JY-23** crystallizes in the monoclinic  $P2_1/c$  space group, having a calculated density of  $1.931 \text{ g cm}^{-3}$  at 293 K and four molecules in the unit cell ( $Z = 4$ ). More detailed crystal data are given in the ESI.† The nitro group at C1 and triazole rings are nearly coplanar, as confirmed by the  $O(1)-N(4)-C(2)-C(1)$  torsion angle of  $-174.8(3)^\circ$ . The trinitomethyl group carbon is  $sp^3$  hybridized, resulting in significant space occupancy. However, **JY-23** has good molecular symmetry, with the trinitomethyl group almost occupying the plane of the triazole ring as the symmetry plane. Based on the given data, the **JY-23** crystal shows a wavelike type packing structure (Fig. 2b) with many strong inter- and intramolecular  $O\cdots O$  interactions between different types of nitro groups, resulting in an excellent density. On the other hand, the shortest non-bonding distance between groups in the molecule is investigated. As illustrated in Fig. 2c, the minimum atomic distance between the trinitomethyl group located at site C and the nitro groups and the trinitomethyl group positioned at site N is  $4.704 \text{ \AA}$ ,  $4.777 \text{ \AA}$ , respectively, and there is almost no repulsion between these groups. The shortest distance between the nitro group and the adjacent trinitomethyl group is  $2.964 \text{ \AA}$ ; it is slightly longer than the shortest distance between nitro

groups in the trinitomethyl group. At the same time, the nitro group at the site C is near the middle of the two nitro groups in the trinitomethyl group, which leads to relatively weak repulsion between the groups and can achieve a certain stability. This phenomenon is supported by the noncovalent interaction (NCI) between **JY-23** groups.<sup>20</sup> The geometric optimization in NCI was accomplished by using the B3LYP6-311G++(d, p) basis set.

To further understand the relationship between the structure and properties, the Hirshfeld surface and 2D fingerprints of **JY-23** were analyzed using Crystalexplorer17.5.<sup>21</sup> As illustrated in Fig. 3, the red spots on the Hirshfeld surface are mainly distributed near the oxygen of the nitro group, indicating strong intermolecular ( $N\cdots O$  &  $O\cdots N$  and  $O\cdots O$ ) interactions. Notably, a prominent spike is observed in the lower left of Fig. 3a and b, representing  $O\cdots O$  interactions.<sup>22</sup> The atomic contact percentages show consistency with the above argument. Among them, the sum of  $N\cdots O$  &  $O\cdots N$  and  $O\cdots O$  interaction accounts for more than 95% and the ratio of  $N\cdots O$  &  $O\cdots N$  interaction is 15%. The high presence of seven nitro groups in **JY-23** implies that the  $O\cdots O$  interaction contributes the most to its Hirshfeld surface with a ratio of 81%, which is the primary cause of its high friction sensitivity ( $FS = 42 \text{ N}$ ).<sup>23</sup>

All relevant physiochemical properties data of **JY-23** are listed in Table 1. The onset decomposition temperature of **JY-23** was determined by differential scanning calorimetry (DSC) at a heating rate of  $5 \text{ K min}^{-1}$  under a  $N_2$  atmosphere to be  $132 \text{ }^\circ\text{C}$  (onset decomposition temperature). It is noteworthy that the thermal

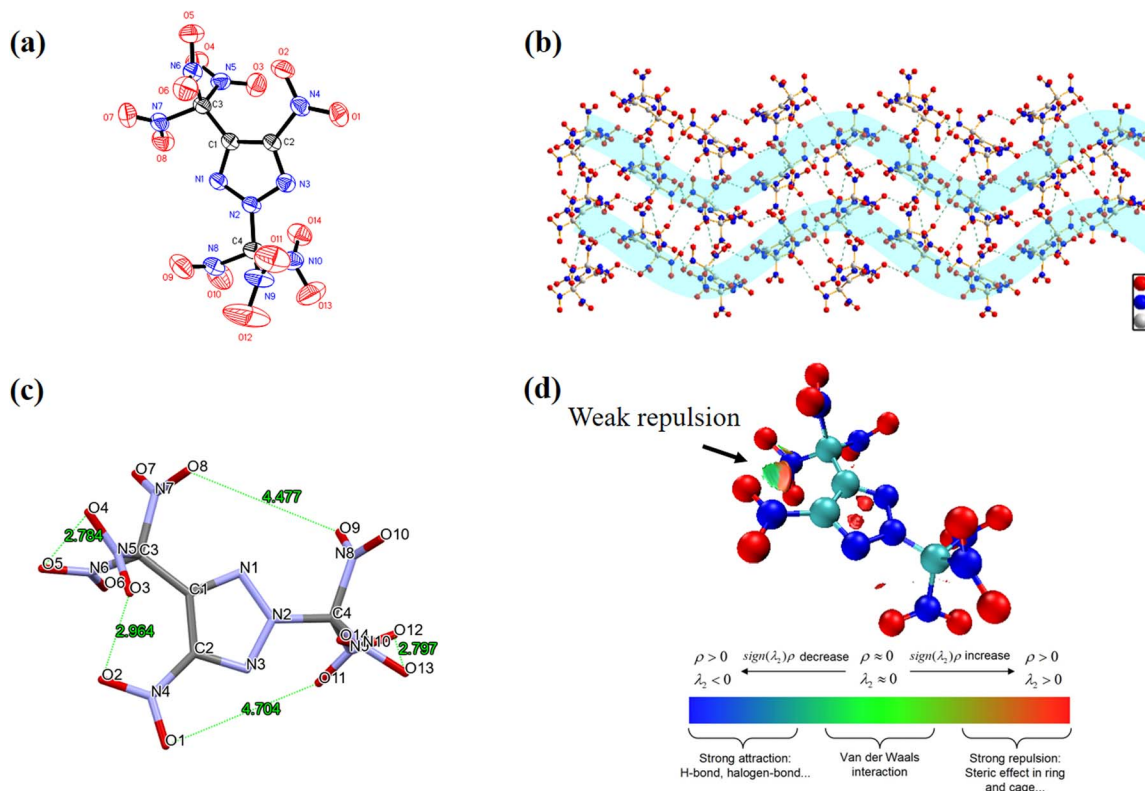


Fig. 2 (a) and (b) Crystal structure of **JY-23**. (c) Crystal packing diagram of **JY-23** along the  $a$  axis. (d) Non-covalent interactions between the groups of **JY-23** (green dashed lines represent  $O\cdots O$  interactions, iso-value = 0.35).



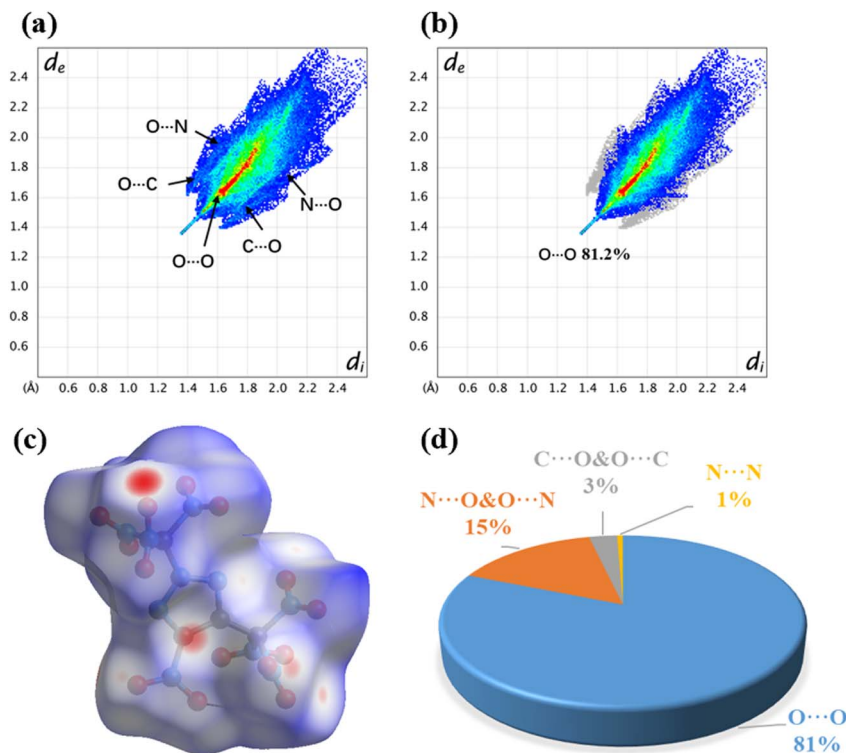


Fig. 3 (a) 2D fingerprint plots in crystal packing found in JY-23. (b) O...O atomic contact percentage contribution to the Hirshfeld surface for JY-23. (c) Hirshfeld surface graph of JY-23. (d) Percentage contributions of the individual atomic contacts to the Hirshfeld surface for JY-23.

Table 1 Physicochemical properties of JY-23 and other oxidizers

| Compounds        | $d^a$ | $T_d^b$ | $\Delta_f H^c$ | $P^d$ | $D_v^e$ | IS <sup>f</sup> | FS <sup>g</sup> | OB <sup>h</sup> | O/O + N <sup>i</sup> |
|------------------|-------|---------|----------------|-------|---------|-----------------|-----------------|-----------------|----------------------|
| JY-23            | 1.931 | 132     | 294.8/0.72     | 31.5  | 8609    | 11              | 42              | +23.3           | 54/88                |
| A <sup>j</sup>   | 1.964 | 160     | 190.2/0.54     | 33.3  | 8761    | 7               | 120             | +18.1           | 55/86                |
| B <sup>k</sup>   | 1.920 | 102     | 29.4/0.08      | 29.2  | 8229    | 4               | 240             | +21.7           | 57/87                |
| C <sup>l</sup>   | 1.900 | 157     | 22.9/0.06      | 30.7  | 8434    | 4               | 120             | +15.3           | 52/86                |
| D <sup>m</sup>   | 1.880 | 73      | 284.3/0.88     | 31.2  | 8511    | 2               | 80              | +17.3           | 50/89                |
| AP <sup>n</sup>  | 1.950 | >200    | -295.8/-2.52   | 15.8  | 6368    | 15              | >360            | +34.0           | 54/65                |
| ADN <sup>o</sup> | 1.808 | 159     | -149.7/-1.13   | 28.9  | 8170    | 4               | 64              | +25.8           | 45/97                |

<sup>a</sup> Density based on single-crystal X-ray diffraction [ $\text{g cm}^{-3}$ ]. <sup>b</sup> Decomposition temperature (onset) under  $\text{N}_2$  [ $5 \text{ K min}^{-1}$ ]. <sup>c</sup> Heats of formation [ $\text{kJ mol}^{-1}/\text{kJ g}^{-1}$ ]. <sup>d</sup> Detonation pressure (calculated with EXPLO5 V6.05) [GPa]. <sup>e</sup> Detonation velocity (calculated with EXPLO5 V6.05) [ $\text{m s}^{-1}$ ]. <sup>f</sup> Impact sensitivity [J]. <sup>g</sup> Friction sensitivity [N]. <sup>h</sup> Oxygen balance (based on  $\text{CO}_2$ ) for  $\text{C}_a\text{H}_b\text{O}_c\text{N}_d$ ,  $1600(c - 2a - b/2)/M_w$ ,  $M_w$  = molecular weight [%]. <sup>i</sup> Oxygen content and combined nitrogen and oxygen content [%]. <sup>j</sup> Ref. 2. <sup>k</sup> Ref. 3. <sup>l</sup> Ref. 15. <sup>m</sup> Ref. 5. <sup>n</sup> Ref. 6. <sup>o</sup> Ref. 7.

stability of JY-23 is higher than that of most of the reported trinitromethyl compounds (Fig. 4c). In addition, the chemical stability of JY-23 was also investigated. JY-23 exhibits good chemical stability in air at room temperature. The physical description of JY-23 is a white solid, and after being placed in the air for a long time, its properties have not changed. At the same time, the weight of JY-23 remains almost unchanged. Finally, JY-23 solids placed in the air were monitored by IR spectroscopy to further verify their chemical stability. As shown in Fig. S20,† the IR spectrum of JY-23 is almost unchanged after 24 h.

The enthalpy of formation of JY-23 was calculated by using the G4(MP2) method<sup>24–28</sup> with the Orca 5.0.3 and pople Python package.<sup>29</sup> JY-23 exhibits a high positive enthalpy of formation

of +294.81  $\text{kJ mol}^{-1}$ , which is higher than that of other nitrogen-rich single heterocyclic compounds. The detonation properties of JY-23 were calculated using the EXPLO5 program (V6.05) based on the density of JY-23 at 293 K.<sup>30</sup> JY-23 exhibits an excellent detonation velocity ( $D_v = 8609 \text{ m s}^{-1}$ ) and detonation pressure ( $P = 31.5 \text{ GPa}$ ). Furthermore, JY-23 demonstrates a superior oxygen balance of +23.3% based on  $\text{CO}_2$ , surpassing that of the heterocyclic oxidizers reported so far and quite close to that of ADN (ammonium dinitramide, +25.8%).

The impact and friction sensitivities of JY-23 were carefully measured by using standard BAM methods. JY-23 shows a comparatively low impact sensitivity of 11 J, while the friction sensitivity was high (42 N).



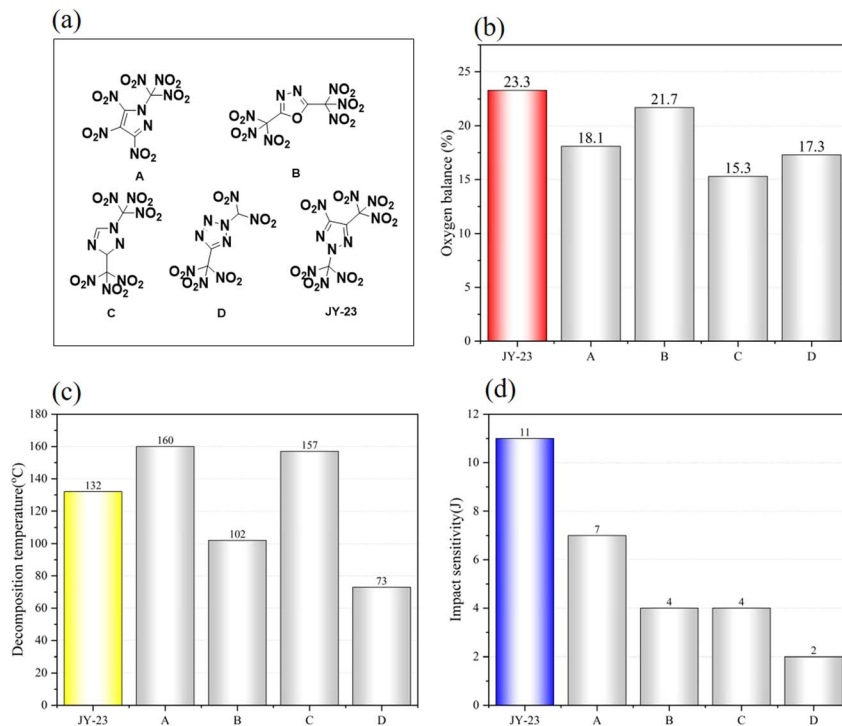


Fig. 4 (a) Reported single heterocyclic oxidizers and **JY-23** prepared in this work. (b–d) The partial property comparison of **JY-23** with other oxidizers.

This is attributed to the large number of O...O interactions in the crystal packing.<sup>31</sup> The electrostatic potential (ESP) on the molecular surface was obtained *via* Multiwfn.<sup>20</sup> Strong positive ESP is known to result in high sensitivity of an energetic compound.<sup>32,33</sup> Analysis of the ESP calculation results (ESI, Fig. S21†) reveals that **JY-23** exhibits uniform charge distribution as the minimum ESP is  $-14.387 \text{ kJ mol}^{-1}$  and the maximum ESP is  $+52.392 \text{ kJ mol}^{-1}$ . Therefore, **JY-23** has a relatively low impact sensitivity (IS = 11 J).

As shown in Fig. 4a, some stable single-heterocyclic oxidizers with the highest oxygen balance have been synthesized based on other azole rings. However, **JY-23** surpasses them with the highest oxygen balance and excellent stability. Although its impact sensitivity is slightly higher, its thermal stability remains moderate. A few organic oxidizer molecules with better thermal stability and slightly higher density exist, but their oxygen balance is much lower. On balance, **JY-23** shows great potential for propellant oxidizers.

To investigate the possible application of **JY-23** in solid propellants, the energetic properties of **JY-23** in HTPB and GAP propellants were estimated by using NASA-CEA<sup>34</sup> and compared with those of three selected heterocyclic oxidizers **A**, **B** and **C** in detail. Here,  $\text{AP}_{68\%}/\text{HTPB}_{14\%}/\text{Al}_{18\%}$  was used as the basic formula to examine the impact of substituting AP with heterocyclic oxidizers. As shown in Fig. 5a, with increasing weight content of heterocyclic oxidizers, the specific impulse showed a general trend of first increasing and then decreasing. Compared with oxidizers **A**, **B** and **C**, **JY-23** has obvious advantages in the specific impulse of HTPB propellants. Oxidizers **A**

and **B** are capable of substituting 25% of AP, reaching the maximum specific impulse of 267.3 s and 266.7 s respectively. It is worth noting that although **B** has a higher oxygen balance than **A**, the lower enthalpy of formation of **B** may explain why the specific impulse of **A** is higher than that of **B**. Only 20% of AP can be replaced by oxidizer **C**, and the maximum specific impulse is 266.0 s. Due to the excellent oxygen balance of **JY-23**, the AP replacement ratio can reach 30% and the maximum specific impulse can reach 268.6 s, which is 3.1 s higher than that of the basic formula. Hence, **JY-23** cannot fully substitute AP in HTPB propellants, but it can be used as an auxiliary oxidizer to adequately substitute some of AP to improve the specific impulse of HTPB propellants.

Specific impulse calculations were carried out using  $\text{AP}_{62\%}/\text{GAP}_{20\%}/\text{Al}_{18\%}$  as the basic formula. It was observed that heterocyclic oxidizers have better energy performance in GAP propellants. Fig. 5b depicts that as the weight percentage of heterocycle oxidizers increases, only oxidizer **C** reaches the maximum specific impulse value (270.4 s) when the substitution amount is 55% due to its lower oxygen balance of +15.3% compared to other oxidizers (**JY-23**: +23.3%; **A**: +18.1%; **B**: +21.7%). The specific impulse of **B**, **C** and **JY-23** enhances as their content increases. **JY-23**, in particular, proves to be the most effective in enhancing the specific impulse, which is evident in an 8.9 s increase compared to the basic GAP formula using AP as an oxidizer. In general, **JY-23** has potential applications in solid propellants, not only as a green oxidizer to replace AP, but also as a high energy additive. More detailed information can be found in the ESI.†



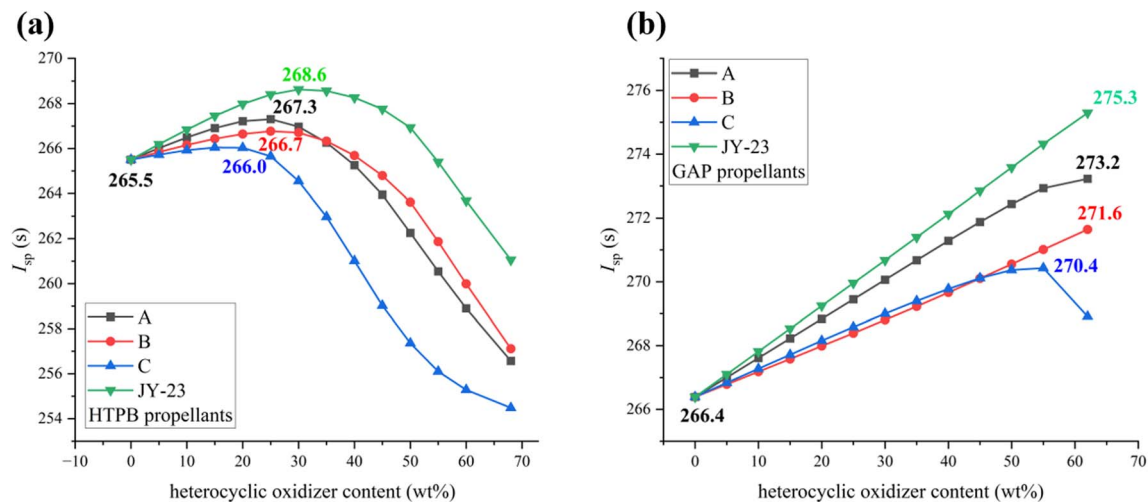


Fig. 5 (a) Calculated  $I_{sp}$  values of HTPB propellants (AP + 18% aluminium + 14% HTPB + heterocyclic oxidizer) at different heterocyclic oxidizer contents. (b) Calculated  $I_{sp}$  values of GAP propellants (AP + 18% aluminium + 20% GAP + heterocyclic oxidizer) at different heterocyclic oxidizer contents.

## Conclusions

In summary, we have designed and synthesized a novel oxidizer 4-nitro-2,5-bis(trinitromethyl)-1,2,3-triazole (**JY-23**) with an oxygen balance of +23.3% through a combination of nitro and trinitromethyl groups and a 1,2,3-triazole ring. Its structure was fully characterized by NMR, IR, elemental analysis, and single-crystal X-ray diffraction. **JY-23** has a high density ( $1.931 \text{ g cm}^{-3}$ ), acceptable thermal stability ( $T_{dec} = 132 \text{ }^\circ\text{C}$ ) and good mechanical sensitivities ( $IS = 11 \text{ J}$  and  $FS = 42 \text{ N}$ ). Additionally, it exhibits good detonation performances ( $D_v = 8609 \text{ m s}^{-1}$  and  $P = 31.5 \text{ GPa}$ ). Significantly, **JY-23** possesses non-hygroscopic properties in contrast to ADN. According to the computation outcomes based on NASA-CEA, replacing AP with **JY-23** will advance the specific impulse in HTPB propellants and GAP propellants. Especially in GAP propellants, the specific impulse can be increased up to 8.9 s. Therefore, **JY-23** is a potential candidate as a green energetic oxidizer to replace AP in solid rocket propellants.

## Author contributions

The manuscript was written through contributions of all authors. All authors have given approval to the final version of the manuscript.

## Conflicts of interest

There are no conflicts to declare.

## Acknowledgements

This work was financially supported by the National Natural Science Foundation of China (NSFC, Grant No. 22175196), the CAS Project for Young Scientists in Basic Research (Grant No. YSBR-052), the Shanghai Science and Technology Committee

(20XD1404800) and the Strategic Priority Research Program of the Chinese Academy of Sciences (Grant No. XDB0590000). Thanks to Dr Li Yao and Jiang Shuaijie for their help in the calculation of this work.

## Notes and references

- I. L. Dalinger, K. Y. Saponitsky, T. K. Shkineva, D. B. Lempert and A. B. Sheremetev, *J. Mater. Chem. A*, 2018, **6**, 14780–14786.
- W. Zhang, Y. Yang, Y. Wang, T. Fei, Y. Wang, C. Sun and S. Pang, *Chem. Eng. J.*, 2023, **451**, 138609.
- Q. Yu, P. Yin, J. Zhang, C. He, G. H. Imler, D. A. Parrish and J. M. Shreeve, *J. Am. Chem. Soc.*, 2017, **139**, 8816–8819.
- Y. Cao, H. Huang, A. Pang, X. Lin, J. Yang, X. Gong and G. Fan, *Chem. Eng. J.*, 2020, **393**, 124683.
- Q. Yu, G. H. Imler, D. A. Parrish and J. M. Shreeve, *Org. Lett.*, 2019, **21**, 4684–4688.
- T. Vo, D. A. Parrish and J. M. Shreeve, *J. Am. Chem. Soc.*, 2014, **136**, 11934–11937.
- K. Mohammad, V. Thaltiri, N. A. Kommu and A. Vargeese, *Chem. Commun.*, 2020, **56**, 12945–12948.
- W. Zhang, J. Zhang, M. Deng, X. Qi, F. Nie and Q. Zhang, *Nat. Commun.*, 2017, **8**, 181.
- J. Li, Y. Liu, W. Ma, T. Fei, C. He and S. Pang, *Nat. Commun.*, 2022, **13**, 5697.
- R. Haiges, G. Bélanger-Chabot, S. M. Kaplan and K. Christe, *Dalton Trans.*, 2015, **44**, 7586–7594.
- V. Thotempudi, H. Gao and J. M. Shreeve, *J. Am. Chem. Soc.*, 2011, **133**, 6464–6471.
- S. Dharavath and J. Zhang, *J. Mater. Chem. A*, 2017, **5**, 4785–4790.
- S. Lal, R. J. Staples and J. M. Shreeve, *Chem. Commun.*, 2023, **59**, 11276–11279.
- G. Zhao, D. Kumar, P. Yin, C. He, G. H. Imler, D. A. Parrish and J. M. Shreeve, *Org. Lett.*, 2019, **21**, 1073–1077.



- 15 Z. Jiang, N. Ding, Q. Sun, C. Zhao, B. Tian, S. Li and S. Pang, *Chem. Eng. J.*, 2023, **473**, 145331.
- 16 H. Gu, Q. Ma, S. Huang, Z. Zhang, Q. Zhang, G. Cheng, H. Yang and G. Fan, *Chem.-Asian J.*, 2018, **13**, 2786–2790.
- 17 L. Liu, Y. Zhang, Z. Li and S. Zhang, *J. Mater. Chem. A*, 2015, **3**, 14768–14778.
- 18 Y. Cao, H. Huang, L. Wang, X. Lin and J. Yang, *J. Org. Chem.*, 2023, **88**, 4301–4308.
- 19 W. Cao, J. Qin, J. Zhang and V. P. Sinditskii, *Molecules*, 2021, **26**, 6735.
- 20 T. Lu and F. Chen, *J. Comput. Chem.*, 2012, **33**, 580–592.
- 21 P. R. Spackman, M. J. Turner, J. J. McKinnon, S. K. Wolff, D. J. Grimwood, D. Jayatilaka and M. A. Spackman, *J. Appl. Crystallogr.*, 2021, **54**, 1006–1011.
- 22 Y. Liu, J. Fan, Z. Xue, Y. Lu, J. Zhao and W. Hui, *Molecules*, 2022, **27**, 4969.
- 23 S. Li, R. Bu, R. Gou and C. Zhang, *Cryst. Growth Des.*, 2021, **21**, 6619–6634.
- 24 F. Neese, *Wiley Interdiscip. Rev.: Comput. Mol. Sci.*, 2012, **2**, 73–78.
- 25 F. Neese, *Wiley Interdiscip. Rev.: Comput. Mol. Sci.*, 2022, **12**, 1606.
- 26 L. A. Curtiss, K. Raghavachari, P. C. Redfern and J. A. Pople, *J. Chem. Phys.*, 1997, **106**, 1063–1079.
- 27 L. A. Curtiss, P. C. Redfern and K. Raghavachari, *J. Chem. Phys.*, 2007, **126**, 084108.
- 28 L. A. Curtiss, P. C. Redfern and K. Raghavachari, *J. Chem. Phys.*, 2007, **127**, 124105.
- 29 E. F. C. Byrd and B. M. Rice, *J. Phys. Chem. A*, 2006, **110**, 1005–1013.
- 30 M. Sućeska, *EXPLO 5, Version 6.05.04*, 2020.
- 31 M. Reichel, D. Dosch, T. M. Klapötke and K. Karaghiosoff, *J. Am. Chem. Soc.*, 2019, **141**, 19911–19916.
- 32 J. Zhang, Y. Feng, Y. Bo, R. J. Staples, J. Zhang and J. M. Shreeve, *J. Am. Chem. Soc.*, 2021, **143**, 12665–12674.
- 33 J. Zhang, Q. Zhang, T. T. Vo, D. A. Parrish and J. M. Shreeve, *J. Am. Chem. Soc.*, 2015, **137**, 1697–1704.
- 34 B. McBride and S. Gordon, *Reference Publication 1311*, NASA, 1996.

